The International Archives of the Photogrammetry, Remote Sensing and Spatial Information Sciences, Volume XLVIII-5/W3-2025
International Conference Applied Photogrammetry and Remote Sensing for Environmental and Industry
„APRSEI – PHEDCS 2025, Tashkent“, 23–25 September 2025, Tashkent, Uzbekistan

A Complex Study of the Kahovka Reservoir Changes After Dam Collapse

Roman Shults

Interdisciplinary Research Center for Aviation and Space Exploration, King Fahd University of Petroleum and Minerals, 34463 Dhahran, Saudi Arabia – roman.shults@kfupm.edu.sa

Keywords: NDVI; Classification; Reservoir; Area; Area Accuracy; Reservoir Coastline; Correlation.

Abstract

The main goal of this research is to develop a comprehensive workflow for using remote sensing data to study the aftermath of a dam collapse. As a case study, the research looks at changes in the Kakhovka reservoir area caused by the dam collapse on June 6, 2023. To evaluate the impact of this disaster, it is essential to analyze key morphometric parameters before and after the failure, the total loss of water surface, changes in soil moisture, and to qualitatively assess the area that has become exposed after water withdrawal; additionally, monitoring land cover changes over the two years following the collapse is vital. The quickest way to do this is by using remote sensing data. The study used Sentinel-2 images from 2020 to 2025. These datasets made it possible to assess changes before and after the dam failure. Image classification before and after the event served as the primary change detection method. Several classification techniques—including random forest, support vector machine, and naïve Bayes—were tested for this purpose. The results showed that support vector machines provided the most effective classification approach for this area. Remote sensing data enabled the identification of geometric and physical changes in the study region. The findings revealed significant changes in the coverage of the Kakhovka reservoir since 2023. The total size of the reservoir was estimated to have decreased substantially. NDVI analysis showed the distribution patterns, and similarities between NDVI profiles were calculated. The areas cleared of water have become vegetated by various tree species and shrubs, indicating a significant shift in the surrounding ecosystem.

1. Introduction

The hydro energy industry plays a vital role in the economy of industrial countries. The energy produced by hydropower plants is relatively inexpensive and environmentally friendly compared to heat-based power stations. However, constructing hydropower stations poses significant environmental risks due to the need to flood large areas of land. Once the reservoir is filled, the surrounding ecosystem adapts to the new environment. Nevertheless, if a dam of a hydropower station collapses, the environmental damage exceeds the impact of the initial construction. The ecosystem suffers from a sudden drop in water levels. Since the reservoir covers a large area, remote sensing data is the most effective tool for monitoring.

Remote sensing data have been used for monitoring large water bodies for many years (Büchele et al., 2006). The open data from Landsat or Sentinel missions have supported numerous studies. The spatial resolution of these data is suitable for most applications since water body monitoring rarely requires accuracy higher than 10 m. Additionally, the spectral bands of these satellites enable in-depth investigations of qualitative imagery parameters (Huang et al., 2018; Rahman et al., 2025). Therefore, the use of remote sensing data is highly prioritized for seacoast and flood monitoring (de Ruiter et al., 2017; Shults et al., 2025), water reservoir changes, and related applications. Recently, many studies have been conducted on similar topics. Notable examples include the use of Sentinel and Landsat data for flood and water resource monitoring (Hussein et al., 2019), supporting water disaster response and recovery (Shah et al., 2023), water monitoring and sanitation interventions (Andres et al., 2018), and volumetric analysis of water reservoirs (Bhagwat et al., 2019).

The paper examines the changes in the Kahovka reservoir area caused by the Kahovka dam collapse on June 6, 2023. To assess the damage from this catastrophic event, it is important to know the main morphometric parameters, specifically the total water loss, and to evaluate the conditions of the area that has been drained. The most efficient way to do this is through the use of remote sensing data.

The paper consists of five sections. Section 2 provides a brief historical overview of the object and data used in the study. The next section describes the classification results for the study area before and after the disaster, along with the total decrease in water surface. Section 4 focuses on the qualitative analysis of changes from 2020 to 2025. This analysis includes a temporal and spatial NDVI study, as well as an investigation of NDVI profiles to assess their similarity and correlation over the years. Visual comparisons showing changes in the Dnipro River coastline after the dam collapse are presented. The final section deals with conclusions.

2. Study object: Kahovka Reservoir, History, and Current State

The idea of constructing a dam downstream of the Dnipro River was proposed many years ago. The primary reason was the presence of a nearly 100 km stretch of rapids near the modern city of Zaporizhzhia, which hindered shipping from the northern part of the country to the Black Sea. The name Zaporizhzhia in Ukrainian means “city that is placed after rapid.” Consequently, the first dam and hydropower station, “Dniproges,” was built in 1932. Its construction enabled navigation along the entire length of the Dnipro River to the Black Sea. After World War II, the Soviet government adopted an ambitious “nature transformation” plan. According to this plan, it was decided to build a system of dams and reservoirs on the Dnipro River (Fig. 1).

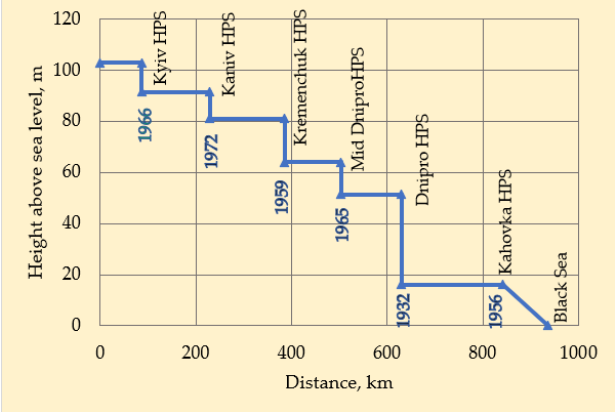

Figure 1. Longitudinal profile of the Dnipro River upstream and the dams that were built.

Since 1955, six hydropower stations and their maintenance reservoirs have been constructed: Kyiv station (1966), Kaniv station (1972), Kremenchuk station (1959), Middle Dnieper power plant (1965), Dnipro station (1932, rebuilt in 1947), and Kakhovka station (1956). The Kahovka Reservoir was created to support the Kahovka station and was filled in 1958. It covered a total area of 2155 km², stretched 240 km in length, with an average width of 23 km. The average depth was 8.4 meters, and its total water volume was about 18.2 km³. The reservoir also supported agriculture in southern Ukraine and supplied water to major cities such as Kherson, Kryvyi Rih, Nova Kahovka, and the Crimean Republic. During the Russian-Ukrainian conflict, the station and dam were seized by the Russian army and were not adequately controlled by either side. After numerous shellings, on the morning of June 6th, 2023, the dam's central part collapsed, causing water to leak. By midday, the dam completely failed, flooding large areas downstream along the Dnipro River (Fig. 2).

Figure 2. UAV imagery of a flooded Kherson after a couple of days of the dam destruction (approx. 10th of June 2023) (CNN, 2023).

In some areas, water reached up to 15 meters. Since the dam failed gradually, the water increased slowly, which helped limit significant damage and loss of life. The estimated number of casualties is around 70 people. However, the full environmental impact is difficult to assess. Large agricultural regions have been flooded, while others have lost their water supply. Hundreds of cities and villages have been affected. The water flowed from the Kahovka reservoir and downstream areas in July 2023, so a final assessment of this disastrous event is still pending.

3. Study of Water Surface Change

3.1 Area Classification Before and After the Dam Collapse

To assess the loss of the reservoir water surface, a change detection algorithm must be applied. Based on the analysis conducted in (Shults et al., 2025), the classification approach for change detection has been chosen. The classification was performed using two Sentinel-2 mosaics: before the dam collapse (01/05/2023-01/06/2023) and after the dam collapse (01/07/2023-01/08/2023). Figures 3 and 4 clearly illustrate the changes in the study area resulting from the dam's collapse.

Figure 3. Color mosaic of Sentinel-2 images of the study area (May 2023).

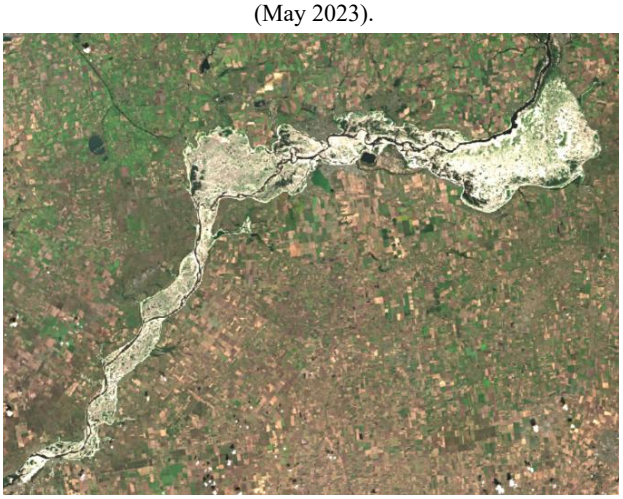

Figure 4. Color mosaic of Sentinel-2 images of the study area (August 2023).

Google Earth Engine (GEE) was used as the primary tool for classification and NDVI calculation. Different classification algorithms were tested. The classification was performed using machine learning algorithms with a sample split into training and testing subsets. The holdout percentage for train/test subsets was set to 70%. The comparison analysis showed the highest efficiency for the support vector machine (SVM) algorithm, compared to random forest and naïve Bayes. Below, the classification results with accuracy estimates are provided.

The area was classified into five classes: water, vegetation, grass, urban, and barren or plowed lands. The last class was selected since the area around the reservoir is mainly used for farming. As a result, a large portion of the land is plowed or harvested during late summer. Figure 5 shows the area classification before the dam collapse.

Figure 5. Area classification before the dam collapse (blue - water, green - vegetation, light green - grass, red - urban, light purple - barren)

The accuracy of the classification is shown in Table 1.

Class	Producer accuracy	User accuracy	F1
Water	0.993	1.000	0.996
Vegetation	0.975	0.912	0.942
Grass	0.963	1.000	0.981
Urban	0.811	0.845	0.828
Barren/Plowed	0.924	0.912	0.918

Table 1. Accuracy of classification before collapse.

The overall accuracy is relatively high at 0.934, and the kappa value is close to one, at 0.917. The estimated reservoir area was 2228.8 km². The classification results for the area after the dam collapse are shown in Fig. 6.

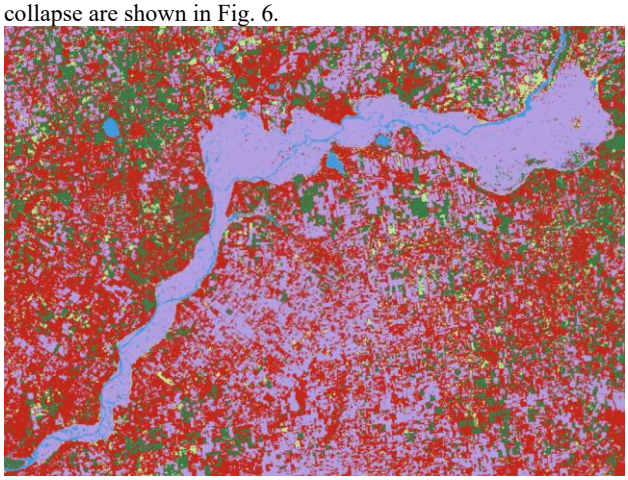

Figure 6. Area classification following the dam collapse.

Visual analysis reveals a significant change across the entire area. While some changes resulted from agricultural activity, the main difference is the dramatic reduction in the reservoir's surface area. These changes complicate classification. However, water classification still maintains very high accuracy, which is crucial for the study. The overall accuracy analysis is provided in Table 2.

Class	Producer accuracy	User accuracy	F1
Water	1.000	1.000	1.000
Vegetation	0.940	0.843	0.889
Grass	0.813	0.888	0.849
Urban	0.664	0.780	0.717
Barren/Plowed	0.952	0.874	0.911

Table 2. Accuracy of classification after the collapse.

The overall accuracy remains relatively high at 0.879, and the kappa value is 0.848. The lowest accuracy is found in the grass and urban classes. However, these classes occupy a tiny part of the study area, so they have no impact on the final estimate. The water surface area is 435.1 km².

3.2 Water Surface Change and Area Accuracy

Based on classification results, the total water surface change is -1793.7 km². Therefore, when comparing this value with the designed water surface area, the initial water surface area before filling the reservoir was 361.3 km². The resulting difference of +73.8 km² is caused by reservoir coastline erosion. These changes contributed to the gradual increase in area over sixty years.

To estimate the reliability of determining an area, it is necessary to calculate the expected area accuracy. The area calculation equation based on point coordinates was used. This equation applies to the area of a closed polygon (1).

$$A = \frac{1}{2}\sum_{i=1}^{n}(X_i Y_{i+1} - Y_i X_{i+1}) , \qquad (1)$$

where X, Y, = coordinates of polygon vertexes

Accepting that coordinates are determined independently with the same accuracy, the expression for the area accuracy will be (2):

$$m_A = \frac{m^2}{4}\sum_{i=1}^{n}[(Y_{i+1} - Y_{i-1})^2 + (X_{i+1} - X_{i-1})^2] , \qquad (2)$$

where m = accuracy of coordinates determination.

Coordinate accuracy, m	Area accuracy, km²	Relative area accuracy
5	0.48	1:4640
10	0.96	1:2320
15	1.44	1:1550
20	1.93	1:1150

Table 3. Simulation of area accuracy.

The table indicates that Sentinel-2 data allow for determining the area with an accuracy of about 1.5-2 km², which is higher than 1:1000 of the total area. Therefore, these data are suitable for similar future studies.

The classification provided geometrical information about the reservoir water surface. However, the primary interest is in qualitative changes that the studied area underwent. Such changes can be estimated by NDVI analysis.

4. NDVI Analysis of the Study Area

4.1 NDVI Distribution Analysis

GEE offers quick and practical tools for NDVI analysis. To examine the changes in the study area, the first step is to create NDVI maps for the investigation period. A series of NDVI maps since the dam collapse provides the best visual understanding. These maps are shown in Figs. 7-9.

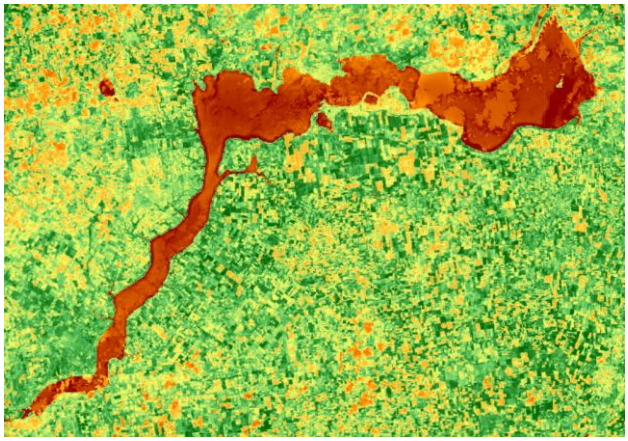

Figure 7. NDVI map of the study area (June 2023).

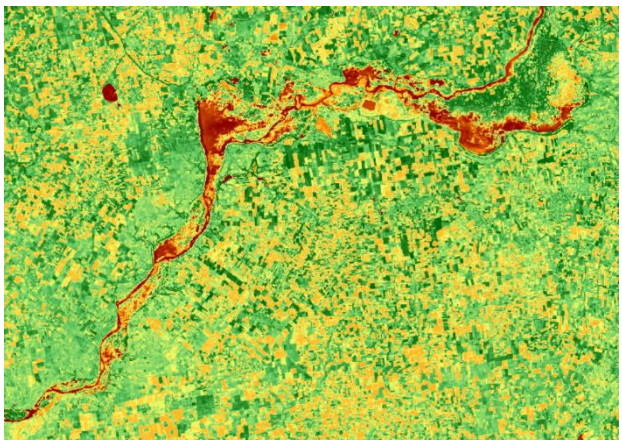

Figure 8. NDVI map of the study area (June 2024).

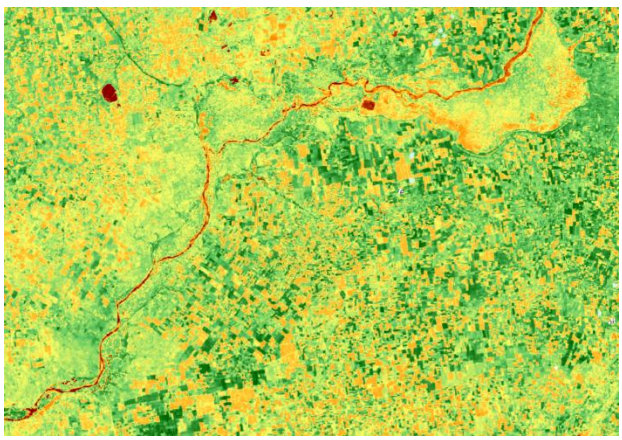

Figure 9. NDVI map of the study area (June 2025).

It is well-known that the NDVI value ranges from -1 to +1. Values from -1.0 to 0.0 correspond to non-vegetated areas such as water, snow, and clouds. Bare soil, sand, or urban surfaces have NDVI values between 0.0 and 0.2, while values from 0.2 to 0.5 represent grasslands, croplands, or shrubs. Dense, healthy vegetation falls within the range of 0.5 to 0.8. Based on these values, the following color palette was used for the NDVI maps: dark brown/red for very low or negative NDVI (water, urban, barren lands), yellow/light green for sparse or stressed vegetation, and green/dark green for healthy, dense vegetation. Using these color designators allows for the analysis of NDVI distribution. The NDVI map for June 2023 (Fig. 7) clearly shows the water reservoir area in brown. Over the course of a year, significant changes occurred (Fig. 8). Part of the former water reservoir became vegetated, particularly in the northeastern part. At the same time, other areas were covered with moderate vegetation and bogs. After another year, the changes were dramatic (Fig. 9). The brown color, indicating bare soil or vegetation-free areas, nearly disappeared everywhere except for the Dnipro riverbed. However, there is a clear trend toward transforming the former reservoir bottom into barren land in the northeastern part. Dark green areas with dense, photosynthetically active vegetation—such as forests or irrigated crops—mostly remained. Nevertheless, the dominant cover was composed of moderate vegetation or grasslands, reflected in light green to yellow colors.

4.2 NDVI Trend Analysis

A single NDVI map shows the current state of vegetation. Despite its clear visual presentation, maps can make NDVI trend analysis somewhat complicated. To address this, trend maps were created. A trend map illustrates the direction of NDVI change over the study period. Usually, NDVI change is shown as greening versus browning. For each pixel with an NDVI value at the observation time, GEE fits a linear regression that relates NDVI values to time (in years). The slope of this regression line indicates the NDVI change (ΔNDVI) per year. A positive slope signifies vegetation “greening” (NDVI increasing over time), while a negative slope indicates vegetation “browning” (NDVI decreasing). Values close to zero suggest a stable NDVI trend.
In the study, two NDVI trend maps were created. The first map shows the NDVI trend for 2020-2023 before the dam collapse. The second map covers the period from 2023 to 2025, after the dam collapse.
Figure 10 demonstrates the NDVI slope map before the dam collapse for 2020-2023.

Figure 10. NDVI slope map for 2020-2023.

The map in Fig. 10 displays ΔNDVI as a continuous variable. This shows how quickly NDVI is changing, including both minor and major fluctuations. A drawback is that a slight positive slope might not be significant due to noise. A strong negative slope clearly indicates browning. For better visualization, the slope map was classified into three classes. The classification used a simple rule, assigning a threshold (T) around zero slope based on the scheme: slope $\leq -T$ indicates browning; $-T \leq$ slope $\leq +T$ indicates stability; slope $> +T$ indicates greening. The T value was set at 0.005 NDVI per year. This facilitated the creation of a clearer and visually appealing map (Fig. 11).

https://doi.org/10.5194/isprs-archives-XLVIII-5-W3-2025-117-2025

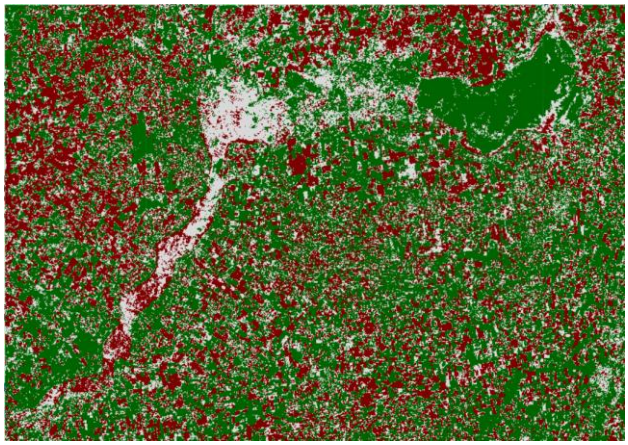

Figure 11. Classified NDVI slope trend map for 2020-2023.

The browning areas indicate where the NDVI trend slope is negative, meaning vegetation cover is decreasing over time (plants dying, deforestation, urban expansion, soil exposure, drought stress, etc.). The stable class (grey) has an NDVI trend slope close to zero, showing no significant change in vegetation. The greening class indicates a positive NDVI trend slope, signifying increasing vegetation cover (reforestation, water greening, crop expansion, improved land use, seasonal recovery, etc.). Therefore, there is no severe stress during the observation period from 2020 to 2023. Using the classified map, the areas of the different NDVI trends were calculated (Table 3).

Class	Browning	Stable	Greening
Area, km²	5516	5673	8262

Table 3. NDVI trend areas by class (2020-2023).

Approximately 5500 km² of land has experienced a consistent decline in NDVI over the time period. Nearly the same area shows no significant NDVI change and remains within natural variability. A larger portion of the land, 8262 km², exhibits a positive NDVI trend, indicating healthier or denser vegetation.
Additionally, the mean NDVI values for each observation epoch were calculated (Fig. 12).

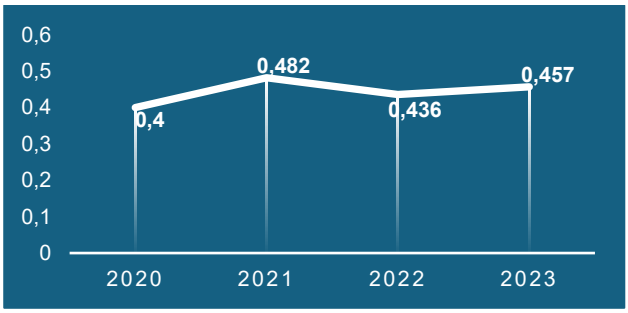

Figure 12. Mean NDVI values per observation epochs 2020-2023.

The average NDVI values stay stable with minor fluctuations caused by weather variability.
To compare the changes that occurred after the dam collapse, the same calculations were performed for the observation period 2023-2025 (June – July). The continuous NDVI slope map is shown in Fig. 13. This figure demonstrates how significantly the water reservoir area and the surrounding land have changed. The reservoir area has become vegetated, while the surrounding land is experiencing water scarcity. Similar to the previous case, the NDVI slope map was classified using a threshold value T (Fig. 14).

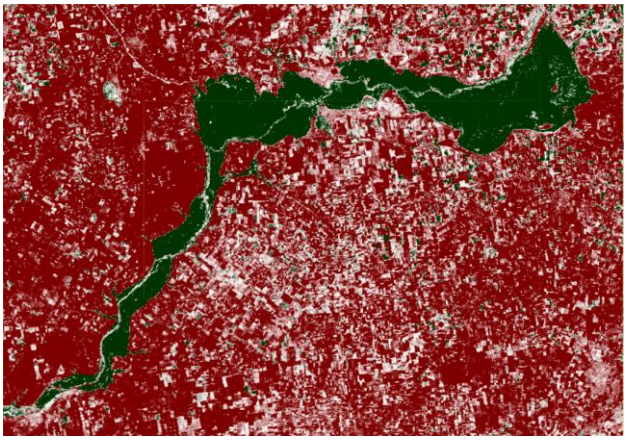

Figure 13. NDVI slope map for 2023-2025.

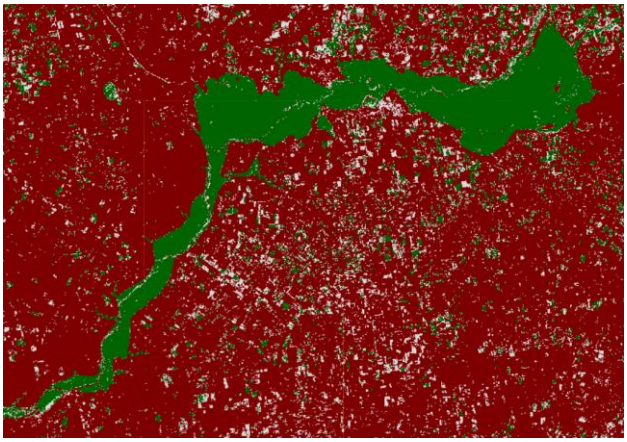

Figure 14. Classified NDVI slope trend map for 2023-2025.

The areas calculated for browning, stable, and greening classes are shown in Table 4.

Class	Browning	Stable	Greening
Area, km²	14233	2052	3166

Table 4. NDVI trend area by class (2023-2025).

Browning is the largest class (≈ 14,200 km²). Greening (≈ 3,200 km²) is nearly equal to stable (≈ 2,100 km²) and has decreased by approximately 64% and 62%, respectively. The balance between vegetation and barren lands has been significantly disrupted. Mean NDVI values per observation epochs were also calculated (Fig. 12).

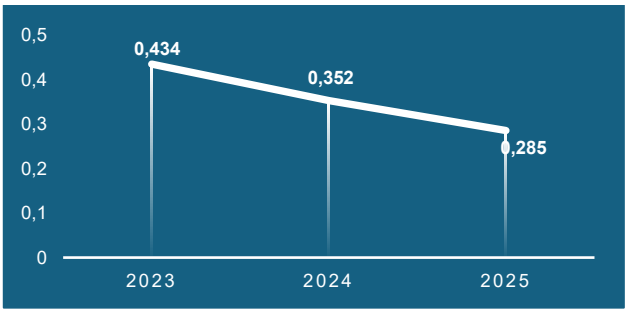

Figure 15. Mean NDVI values per observation epochs 2023-2025.

The calculated mean NDVI values also declined significantly. If the average NDVI value for 2020-2023 is 0.444, then for 2023-2025 it dropped to 0.285, or 35%, which is an unusually low value.

4.3 NDVI Similarity Estimation

The final step is to conduct a direct study of the empty water reservoir. This study will help understand the changes that occurred on the reservoir bottom. A total of seven cross-sections were drawn (Fig. 16).

Figure 16. Cross-section distribution over the former reservoir.

For each cross-section, NDVI profiles were generated with a 100 m step. Therefore, each chart contains six profiles corresponding to yearly June-July observation periods. Examples of these charts are shown in Figs. 17 and 18. For improved interpretability, NDVI profiles were smoothed using a 200 m smoothing window.

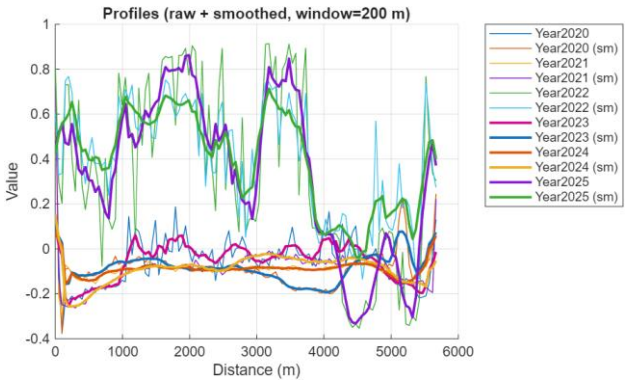

Figure 17. Cross-section 1.

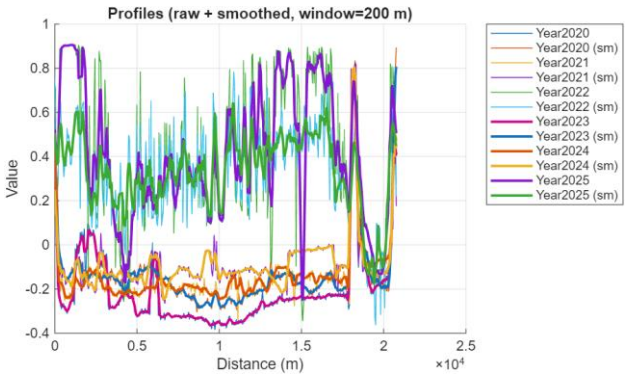

Figure 18. Cross-section 7.

For each chart containing NDVI profiles, the similarity analysis was conducted. The following parameters were calculated: Pearson correlation, cosine similarity, Euclidean distance, root mean square errors (RMSE), lag versus similarity charts, and correlation versus cosine similarity graphs. The most informative are heatmaps that demonstrate the correlation between charts in the NDVI profile and temporal correlation graphs. Examples of the correlation heatmaps are provided in Figs. 19 and 20.

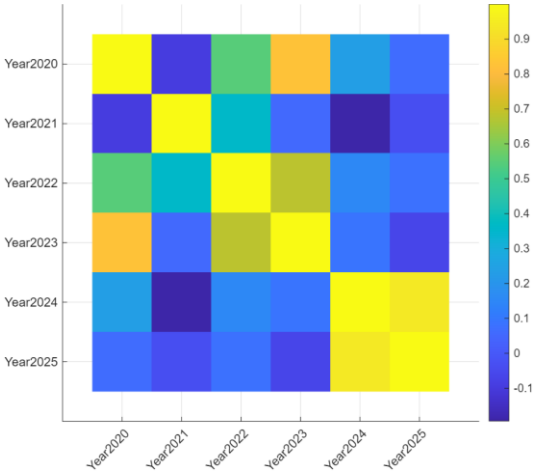

Figure 19. Pearson correlation for cross-section 1.

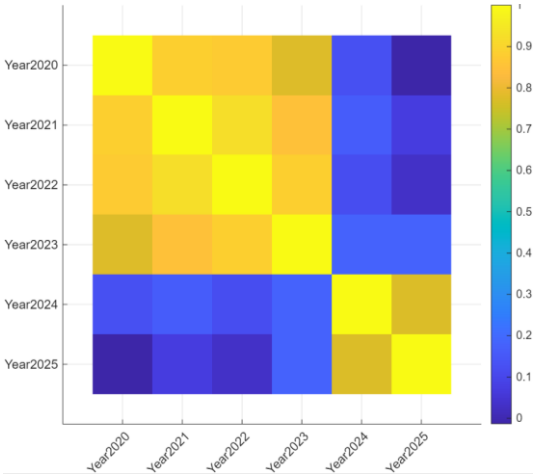

Figure 20. Pearson correlation for cross-section 7.

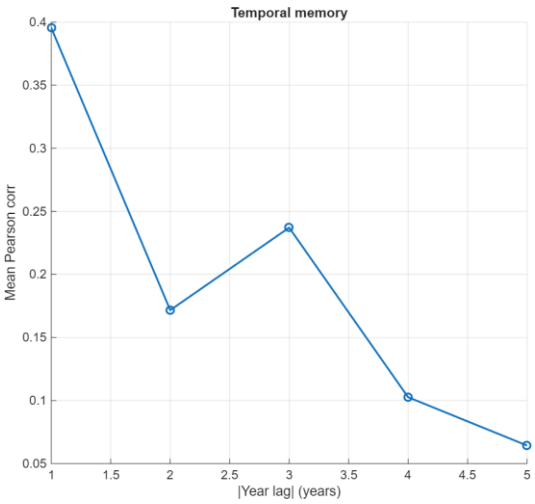

Figure 21. Temporal correlation for cross-section 1.

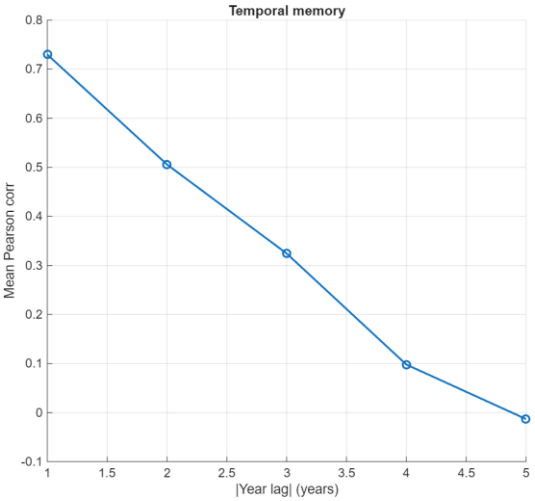

Figure 22. Temporal correlation for cross-section 7.

The analysis reveals distinct profiles divided into two datasets: 2020-2023 and 2024-2025. The correlation analysis shows an extremely high correlation (0.9-0.7) between 2020-2023 and a nearly negligible correlation (0.2-0.1) between 2020-2023 and 2024-2025 (see Figs. 19-20), with a strong correlation between 2024 and 2025. The same conclusions apply to cosine similarity, with values 0.9-1.0 for 2020-2023 and -0.4 to -0.8 for 2024-2025. The distribution of Euclidean distances and RMSEs confirms the differences between these two datasets. The charts showing changes in mean Pearson correlation over time indicate a rapid decline after the third year, which is 2023. Consequently, the analysis demonstrates significant changes in land surface coverage for the former reservoir bottom.

5. Conclusions

The study presents the results of exploring changes in the Kahovka reservoir following the dam collapse and their environmental impact. The proposed change detection strategy enables the determination of change distribution after the dam failure and allows for both qualitative and quantitative estimates of the changes. The geometric assessment of water surface reduction was performed using Sentinel-2 imagery classification for different observations before and after the dam collapse. At this stage, SVM classification combined with comparison using GEE was completed. Thanks to detailed classification validation through the confusion matrix, the accuracy of the classification and water surface area measurements was evaluated. A qualitative assessment was also obtained through various NDVI comparisons. Calculations of NDVI values, their differences, trends, and cross-sections were carried out using GEE. Since the main consequences involved vegetation cover loss and irrigation changes, NDVI proved to be the best indicator, highlighting regions where vegetation changes occurred. The NDVI cross-section analysis showed distinct profiles split into two datasets—before and after the dam collapse. Pearson correlation, cosine similarity, Euclidean distance distributions, and the relationship between Pearson correlation and time lag confirmed this difference.

Future research will need to examine the use of other indices to investigate changes in the area of the former Kahovka reservoir. Additionally, more comprehensive monitoring results will be gathered for the study of the seasonal dynamics of the reservoir.

References

Büchele, B., Kreibich, H., Kron, A., Thieken, A., Ihringer, J., Oberle, P., Merz, B., Nestmann, F., 2006: Flood-Risk Mapping: Contributions towards an Enhanced Assessment of Extreme Events and Associated Risks. *Nat. Hazards Earth Syst. Sci.* 2006, 6, 485–503. https://doi.org/10.5194/nhess-6-485-2006

Huang, C., Chen, Y., Zhang, S., Wu, J., 2018: Detecting, Extracting, and Monitoring Surface Water from Space Using Optical Sensors: A Review. *Reviews of Geophysics*, 56, 333-360. https://doi/10.1029/2018RG000598

Rahman, M.M., Shults, R., Tiwari, S.P., Arshad, A., Usman, M., Raihan, A., Ishraque, M.F., 2025: Review on sea water quality (SWQ) monitoring using satellite remote sensing techniques (SRST). *Marine Pollution Bulletin,* 217, 118108. https://doi.org/10.1016/j.marpolbul.2025.118108

de Ruiter, M.C., Ward, P.J., Daniell, J.E., Aerts, J.C.J.H., 2017: A Comparison of Flood and Earthquake Vulnerability Assessment Indicators. *Nat. Hazards Earth Syst. Sci*. 17, 1231–1251. https://doi.org/10.5194/nhess-17-1231-2017

Shults, R., Farahat, A., Usman, M., Rahman, M.M., 2025: Multi-Temporal Remote Sensing Satellite Data Analysis for the 2023 Devastating Flood in Derna, Northern Libya. *Remote Sensing*, 17(4), 616. https://doi.org/10.3390/rs17040616

Hussein, S., Abdelkareem, M., Hussein, R., Askalany, M., 2019: Using Remote Sensing Data for Predicting Potential Areas to Flash Flood Hazards and Water Resources. *Remote Sens. Appl. Soc. Environ*. 16, 100254. https://doi.org/10.1016/j.rsase.2019.100254

Shah, A., Kantamaneni, K., Ravan, S., Campos, L.C., 2023: A Systematic Review Investigating the Use of Earth Observation for the Assistance of Water, Sanitation and Hygiene in Disaster Response and Recovery. *Sustainability*, 15, 3290. https://doi.org/10.3390/su15043290

Andres, L., Boateng, K., Borja-Vega, C., Thomas, E., 2018: A Review of In-Situ and Remote Sensing Technologies to Monitor Water and Sanitation Interventions. *Water* 2018, 10, 756. https://doi.org/10.3390/w10060756

Bhagwat, T., Klein, I., Huth, J., Leinenkugel, P., 2019: Volumetric Analysis of Reservoirs in Drought-Prone Areas Using Remote Sensing Products. *Remote Sens.*, 11, 1974. https://doi.org/10.3390/rs11171974

CNN, 2023: In pictures: The collapse of Ukraine's Nova Kakhovka dam. https://edition.cnn.com/2023/06/07/world/gallery/ukraine-nova-kakhovka-dam-collapse. (27 August 2025).